



HHS Public Access

Author manuscript

Lab Invest. Author manuscript; available in PMC 2010 April 20.

Published in final edited form as:

Lab Invest. 2009 September ; 89(9): 1007–1017. doi:10.1038/labinvest.2009.58.

Osteopetrosis with Micro-lacunar Resorption due to Defective Integrin Organization

Harry C Blair^{1,2}, Beatrice B Yaroslavskiy², Lisa J Robinson², Markus Y Mapara³,
Alessandra Pangrazio^{4,5}, Lida Guo², Ka Chen², Paolo Vezzoni^{4,5}, Jakub Tolar⁶, and Paul J Orchard⁶

¹Department of Pathology, University of Pittsburgh, and Veteran's Affairs Medical Center, Pittsburgh, PA 15243

²Department of Cell Biology and Physiology, University of Pittsburgh, and Veteran's Affairs Medical Center, Pittsburgh, PA 15243

³Department of Medicine, University of Pittsburgh, and Veteran's Affairs Medical Center, Pittsburgh, PA 15243

⁴Istituto di Tecnologie Biomediche, CNR, Segrate, Italy

⁵Istituto Clinico Humanitas, IRCCS, Rozzano, Italy

⁶Department of Pediatrics, Division of Blood and Marrow Transplantation, University of Minnesota, Minneapolis, MN 55455

Abstract

We used in vitro differentiation of monocytes to characterize the cellular defect in a type of osteopetrosis with minimally functional osteoclasts, where defects associated with common causes of osteopetrosis were excluded by gene sequencing. Monocytes from blood of a 28 year old subject were differentiated in media with RANKL and CSF-1. Cell fusion, acid compartments within cells, and TRAP activity were normal. However, the osteoclasts made abnormally small pits on dentine. Phalloidin labeling showed that the cell attachments lacked the peripheral ring structure that supports lacunar resorption. Instead, the osteoclasts had clusters of podosomes near the center of cell attachments. Antibody to the $\alpha\beta 3$ integrin pair or to the C-terminal of $\beta 3$ did not label podosomes, but antibody to αv labeled them. Western blots using antibody to the N-terminal of $\beta 3$ showed a protein of reduced size. Integrins $\beta 1$ and $\beta 5$ were upregulated, but, in contrast to observations in $\beta 3$ defects, $\alpha 2$ was not increased. The rho GTP exchange protein Vav3, a key attachment organizing protein, did not localize normally with peripheral attachment structures. Vav3 forms of 70 kD and 90 kD were identified on Western blots. However, the proteins $\beta 3$ integrin, Vav3, Plekhm1 and Src, implicated in attachment defects, had normal exon sequences. In this new type of osteopetrosis, the integrin organizing complex is dysfunctional, and at least two attachment proteins may be partially degraded.

Users may view, print, copy, and download text and data-mine the content in such documents, for the purposes of academic research, subject always to the full Conditions of use:http://www.nature.com/authors/editorial_policies/license.html#terms

Correspondence: Harry C Blair MD, 705 Scaife Hall, Pittsburgh, PA 15261, Tel 412 383-9616 Fax 412-647-8567, htblair@imap.pitt.edu.

Keywords

Osteopetrosis, Bone resorption; Integrin assembly; Receptor activator of NF- κ B; rho GTPase

Introduction

Genetic disorders that compromise bone degradation cause osteopetrosis [1]. Without remodeling of mineralized cartilage and bone, long bones are packed with mineralized matrix. Mature lamellar bone cannot replace woven bone, causing a high frequency of fractures. Fractures heal poorly and often with deformity. In severe cases, the optic nerve is entrapped shortly after birth with consequent blindness. In all but the mildest forms, reduction of bone marrow causes anemia and hepatosplenomegaly due to extramedullary hematopoiesis. Osteopetrosis associated with hematological dysfunction is progressive and may require allogeneic hematopoietic stem cell transplant, which has the capacity to produce osteoclasts capable of remodeling the skeleton.

Osteopetrosis is rare but extensively studied. Most cases of human osteopetrosis have molecular diagnoses. The central activity of the osteoclast is acid transport to dissolve bone mineral, driven by a vacuolar-type H⁺-ATPase [2] one subunit of which is an osteoclast-specific isoform [3]. Mutations in the TCIRG1 gene coding for this isoform are the predominant cause of human osteopetrosis [4]. The v-type H⁺-ATPase is electrogenic, so anion transport must exist to balance H⁺ for the acid secretion that dissolves bone mineral, and a chloride-proton exchanger, CLCN7 [5], is also critical to osteoclast function [6]. Defects in CLCN7 are responsible for many cases of osteopetrosis with normal TCIRG1, including dominant genotypes. CLCN7 requires a second membrane protein for its function, OSTM1 [7]. Another protein required for formation of the acid secreting apparatus is Plekhm1, which by homology is probably a small GTPase of the Ras family [8]. There are other rare causes of sclerotic diseases of bone including defects in acid proteinase activity, and a number of defects in osteoclast differentiation, most known only from knockout mice [9]. However, most cases of osteopetrosis have many nonfunctional osteoclasts, while in rare cases with few or no osteoclasts defects in RANKL, a TNF-family protein that is a key osteoclast differentiation signal, have been identified [10]. On the other hand, studies of organizing proteins of the rho GTP exchange family have shown that Vav3 is required for normal osteoclast attachment, and that Vav3 knockout mice have an osteopetrotic phenotype without major developmental defects in other organ systems [11]. One cause of osteoclast-poor osteopetrosis has recently been shown to be defects in RANK signalling [12].

Despite these advances in the molecular etiology of osteopetrosis, about 20% of cases do not demonstrate any known defect. Some cases have defied systematic classification based on current developmental pathways; this work studies the basis of one such with normal RANK and acid transport, but an osteoclast attachment defect. Osteoclast attachment is mediated by the α v β 3 integrin, and the attachment is linked to complex additional proteins that create a tight annular bone adhesion zone at the periphery of the osteoclast. Without this attachment, bone cannot be acidified and degraded. However, defects in attachment integrins that are not lethal during embryonic development are usually mild due to compensatory expression of

integrins with similar function [13]. Here we describe a form of osteopetrosis that does not fit this paradigm. Osteoclasts could be differentiated *in vitro* and resorb bone. However, the osteoclast podosome distribution was highly disordered, and only very small resorption lacunae were made by the cells. The affected osteoclasts make the αv and $\beta 3$ integrins, but integrin assembly was abnormal, probably due to a defect in the organizing complex affecting its stability.

Materials and Methods

Osteopetrotic cells and genetic sequencing

Cells were from peripheral blood a 28 year old adult osteopetrotic patient; controls used cells from healthy blood donors. The subject was diagnosed at 3 years of age, and developed chronic osteomyelitis of the mandible and left femur and multiple fractures of long bones. Radiographs showed osteosclerosis, and osteopetrosis was confirmed by biopsy. Osteoclasts were present, and common causes of osteopetrosis were excluded by normal *CLCN7* and *TCIRG1* sequences from PCR-amplified cDNA [14], performed as clinical tests (Connective Tissue Gene Tests, Allentown, PA). The subject had normal hemostasis into young adulthood and despite chronic infectious complications was stable with conservative management. Decision to transplant at age 28 was due to progressive splenomegaly, leukoerythroblastosis and thrombocytopenia. Prior to transplant, 40 ml of blood was taken for analysis of osteoclastic function by *in vitro* osteoclast differentiation in a protocol approved by the Institutional Review Board. Further sequencing of gene defects reported to cause defects related to the *in vitro* findings used sequencing of PCR amplified DNA using primer pairs specified in Table I.

Cell Culture

In vitro osteoclast generation used 40 ml of heparin anticoagulated blood. Control osteoclasts were made from citrate anticoagulated buffy coats saved from leukoreduction of donor blood. Mononuclear cells were recovered on ficoll and CD14 osteoclast precursors were enriched using anti-CD14-magnetic microbeads (Miltenyi Biotec, Auburn CA) as described [4]. To induce osteoclast differentiation, media were supplemented with 10 ng/ml CSF-1 and 40 ng/ml recombinant RANKL, and media were changed twice weekly. Cells were grown on glass coverslips in 0.5 cm² wells. For resorption assays, 5 mm diameter whale dentine discs, 1 mm thick, were added to the tissue culture wells. Mononuclear cells recovered on ficoll are approximately 50% CD14 or CD11 monocytes, while CD14 affinity purified cells are approximately 98% monocytes by flow analysis as previously shown [15]. Other cells in ficoll-separated buffy coats include lymphocytes and some polymorphonuclear leukocytes, which do not attach to glass and do not represent significant numbers of cells in fully differentiated osteoclast cultures. Typically, at time of study 50% of cells in cultures are mononuclear, and the remainder are multinucleated osteoclasts, regardless of whether ficoll buffy coat cells or CD14 purified monocytes are used for production. Only the multinucleated, TRAP expressing cells were considered in studies of cell adhesion.

Fluorescent antibody labeling and Western analysis

Anti-vitronectin receptor CD51/CD61 ($\alpha v\beta 3$) mouse monoclonal anti-human 23C6 sc-7312, αv rabbit polyclonal antibody sc-10719, $\beta 1$ (N-terminal anti 20mer, sc-6622) goat anti- $\beta 3$ (N-terminal anti 20mer sc-6627) goat polyclonal antibody, $\beta 3$ C-terminal mouse monoclonal antibody 611140, $\beta 5$ (E19 anti N-terminal peptide, sc-5401) and $\alpha 2$ (N-terminal anti 19mer, sc-6585) were anti-human antibodies. Antibodies to integrins and to the vitronectin receptor were from Santa Cruz (Santa Cruz, CA) except for the $\beta 3$ C-terminal antibody which was from BD Transduction labs (San Jose, CA). Antibody to Vav3 was a goat polyclonal (ab21208) from AbCam (Cambridge, MA) prepared to the synthetic human peptide CSGEQGTLKLPEK and was used at 1 $\mu\text{g/ml}$ for Western blot and 3 $\mu\text{g/ml}$ for immune localization. Other antibodies were used for immune fluorescence at 1:100 dilution and for Western blotting at 1:200. Al-488-conjugated goat anti-mouse or donkey anti-goat second antibodies were from Jackson Immunoresearch (Westgrove, PA), and rhodamine-conjugated phalloidin for labeling filamentous actin was from Molecular Probes (Eugene, OR). Immune fluorescence labeling was as described.¹² For Western blots cell lysates were made using 0.3% SDS, 50 mM tris, pH 7, with proteinase and phosphatase inhibitors. Proteins were separated on 8 or 10% SDS-PAGE and transferred to polyvinylidene membranes. Primary antibodies were, for detection on Western blots, used with alkaline phosphatase-coupled secondary antibodies (Pierce immuno-pure polyclonal antibodies, Thermo-Fisher Inc., Rockford IL) followed by enhanced chemiluminescence detection (ECL plus, Amersham, Piscataway, NJ) as described [16]. Efficiency of osteoclast formation in vitro between control and osteopetrotic precursor cells, using similar densities of attached monocytes appeared to be the same within a factor of two. The fusion efficiency could not be determined more accurately due to the limited number of osteopetrotic precursor cells available.

Enzyme activity, acid transport, and pit assays

Tartrate resistant acid phosphatase (TRAP) was assayed in cells fixed in citrate buffer at pH 5.4 with 40% acetone. Acid phosphatase activity was then determined using naphthol AS-BI phosphate substrate with fast garnet GBC to visualize the product as a red precipitate in 0.67 M tartrate at pH 5.6 (Sigma, St Louis, MO). Acid vesicles in osteoclasts were identified using the fluorescent polyamine-pyrrole dye Lysotracker red DND-99 (Molecular Probes, Eugene, Or), 2.5 μM , added 15 minutes prior to observation. The dye diffuses through membranes at neutral pH. Its amines are protonated at low pH and accumulate in acid compartments, which are not permeable to ions. Lacunar resorption was assessed after 12 days of culture of osteoclasts on slices of whale dentine [17]. The substrate was cleaned by ultrasonic disruption in 1% sodium borate for 5 minutes to remove cell debris. The substrate was then stained for 2 minutes with 1% toluidine blue to label the surface collagen exposed by degradation.

Microscopy

Images were obtained on a Nikon TE2000 inverted phase-fluorescence microscope using a 12-bit 1600 \times 1200 pixel monochrome charge coupled device with an RGB filter wheel for color photographs (Spot Instruments, Sterling Heights, MI). For green fluorescence,

excitation was at 450–490 nm with a 510 nm dichroic mirror and a 520 nm barrier. For red fluorescence (including lysotracker red), excitation was at 536–556 nm with a 580 nm dichroic mirror and a 590 nm barrier. For blue fluorescence, excitation was at 380–425 nm with a 430 nm dichroic filter and a 450 nm barrier. Fluorescent labels were photographed using 1.3 NA 40× or 100× oil objectives.

Results

Features of the osteopetrotic bone

The subject was 28 years old at the time of the study. PCR-based sequencing for defects in TCIRG1 or CLCN7, the common clinical causes of osteopetrosis, was negative. The iliac crest had a markedly abnormal medullary cavity with matrix consisting of calcified cartilage and woven bone (Figure 1A). Although the patient had severe hematological abnormalities including leukoerythroblastosis and thrombocytopenia, the complication of blindness had been avoided. This may be due to residual surface degradative activity. This is supported by the observation at high power of osteoclasts with scalloped lacunae (Fig 1B) that were much smaller than those of normal osteoclasts, which cut lacunae roughly the diameter of the cell.

Osteoclasts differentiated in vitro

Osteoclast CD14 precursors were isolated from blood of the subject and plated on whale dentine or glass, in parallel with control cells from normal blood donors. The osteoclast derived from osteopetrotic mononuclear cells made clear, but very small, pits (Figure 2A) that had on average ~10% of the area of pits from normal cells (Figure 2B). The micro-pits from the osteopetrotic cells resembled micro-lacunar resorption produced by human monocytes in TNF α rather than RANKL [18], but the cells were as extensively multinucleated and spread as normal osteoclasts (Figure 2C), and produced the typical osteoclast enzyme tartrate resistant acid phosphatase (TRAP) in large quantities (Figure 2D). In keeping with the normal sequence of major acid-transport proteins, vacuolar acidification by Lysotracker labeling of acid compartments appeared typical for osteoclasts in vitro (Figure 2E).

Structural anomalies in membranes and attachment structures

At high magnification, osteopetrotic osteoclasts had prominent membrane structures in central regions of the cells (Figure 3A), which did not occur in control osteoclasts. It could not be determined with certainty whether these additional membrane images in phase were within or on the border of the affected cells. Similar structures were seen in phalloidin labeling as large concentrations of actin labeled membranes (Figure 3C), which also revealed large clusters and bands of podosomes, in many cases across the center of the osteoclastic cell attachments. In contrast, normal osteoclasts (Figure 3B,D) had well defined peripheral rings of podosomes, no increased membranes in the cell center on phase, and no irregular bands of phalloidin labeling.

Integrins in osteopetrotic and control osteoclasts

Osteopetrotic cells were labeled for actin with phalloidin (red) and antibodies for the $\alpha v \beta 3$ integrin pair or αv and $\beta 3$ subunits (green), and with Hoechst dye to visualize nuclei (Figure

4 A). The affected cells had prominent podosomes but the distribution of podosomes was abnormal. There were many podosomes in the cell centers, while in normal cells the podosomes are organized in annular rows associated with actin rings. A monoclonal antibody for the $\alpha v\beta 3$ integrin showed no colocalization with podosomes in osteopetrotic cells. Polyclonal antibodies to αv showed colocalization with podosomes (Figure 4A) but $\beta 3$ integrin did not colocalize using antibody to the N-terminus. This and the lack of labeling with the monoclonal antibody recognizing the $\alpha v\beta 3$ integrin pair probably reflect abnormal processing of the $\beta 3$ subunit. That the podosomes in osteopetrotic cells expressed integrins in small central clusters suggested that the integrins are synthesized, but are not trafficked properly or are unstable. In contrast, in control cells all of the integrin antibodies showed excellent podosome colocalization with phalloidin labeling (Figure 4B). Labeling for $\alpha 2$ did not label podosomes in control or osteopetrotic cells (not illustrated).

Organizing complexes for integrin assembly

These findings indicated changes in integrin distribution. The changes in osteoclast function would be consistent with interference with organizing complexes. These are driven by actin and by rho-type GTP exchange factors that regulate adhesion structure assembly and stability. The family of rho GTP exchange factor regulatory proteins includes the Vav (Vav1) oncogene and BRCA1; the Vav3 rho GTP exchange factor was recently discovered to be critical to osteoclast attachment organization [11]. By immune labeling, abundance and distribution of Vav3 labeling in control and osteopetrotic osteoclasts was studied (Figure 5). Surprisingly, Vav3 appeared to be at least as abundant in osteopetrotic and control cells, but unlike the normal Vav3 distribution, which occurs in punctate complexes surrounding podosomes and at actin organizing centers (top right panel), Vav3 in the osteopetrotic osteoclasts lacked specific association with these structures (bottom panels). This suggested an abnormal assembly of the Vav3 complex.

Western blots for integrin subunits and Vav3 in the osteopetrotic osteoclasts

Size and quantity of αv in the osteopetrotic cells matched that of normal osteoclasts (Figure 6). An N-terminal $\beta 3$ antibody detected only small amounts of $\beta 3$ in the osteopetrotic cells (Fig 6 (1)), while a C-terminal antibody showed normal quantities of $\beta 3$ of slightly smaller size (Fig 5 (2)), suggesting that the protein is abnormally processed, or that there is an N-terminal deletion. Possibilities included abnormal $\alpha v\beta 3$ assembly or stability, or a mutation (see below). The cell lysates were studied for alternative α and β chains; $\beta 1$ was greatly increased and $\beta 5$ was somewhat increased in osteopetrotic cells (Fig 6 (3)). HeLa cells, where $\beta 1$ is a major adhesion protein, are shown as a control. MG63 is shown as a control for $\beta 5$ expression. These findings suggested that the osteopetrotic cells responded to some extent by altering integrin synthesis. This also occurs in $\beta 3$ deletion (Glantzmann's thrombasthenia) [13]. However, the abnormal podosome distribution caused a much more serious phenotype than results from $\beta 3$ deletion. In contrast, Western blot for Vav3 [11] showed a minor normal product of ~ 90 kD and a second band, only in osteopetrotic cells, at ~ 70 kD. At this point no new lysate was available; Figures 6 (4) and (5) are re-blots; the Vav3 blot was done in triplicate with identical results (two are shown). Here also, HeLa cells are shown as a control for normal Vav3. In $\beta 3$ defects $\alpha 2$ is also upregulated [13]; in this case, $\alpha 2$ was a minor product and was not clearly increased. The $\alpha 2$ blot Figure 6 (5)

required long exposures relative to other integrins, so it is likely that $\alpha 2$ was a small fraction of α integrin quantity in normal or osteopetrotic cells.

Sequences of genes reported to cause abnormal integrin assembly

Sequences of all exons of $\beta 3$ from the subject's genome matched the normal protein. In addition, all exons of Vav3, Src and Plekhm1, which cause defects in osteoclast attachment organization in animal models (see Discussion) were sequenced. These also matched those of the normal human proteins. For sequencing primers and gene names see Table 1.

Discussion

We characterized osteoclasts from a subject with severe osteopetrosis, surviving to adulthood but requiring transplant for hematopoietic system failure, with abnormal osteoclast attachment. Many attachment proteins are produced by cells of monocyte lineage during differentiation, and, although a number of abnormalities have been described in these attachment proteins, there are no human precedents for the functional defect described here. Most human osteopetrosis is due to defects in the specialized acid secretion apparatus, probably because this relatively recent and specialized function has little overlap with other functions of acid secretion [9]. There are many causes of osteopetrosis related to defective osteoclast maturation, but most are known only from transgenic animals. Clinically these will clearly be very rare, although two forms, related to either RANKL or RANK defect, do occur, and are cause of osteoclast-poor osteopetrosis [10, 12, 19].

Human mononuclear osteoclast precursors occur in the monocyte fraction of marrow and in peripheral blood. They express the integrins CD11b-c and the lipopolysaccharide receptor antigen CD14 [20], but do not express the membrane attachment proteins that characterize mature osteoclasts, principally the vitronectin receptor (the $\alpha v\beta 3$ integrin) [21, 22]. Absence of the αv integrin chain, which is widely expressed and required for normal vasculogenesis, is lethal in the embryonic period [23], while absence of the $\beta 3$ chain causes Glantzmann's thrombasthenia, a defect in platelet adhesion usually with minimal effects on bone degradation. Curiously, the principal substitute integrin pair is $\alpha 2\beta 1$ in the absence of $\beta 3$ [13]. On the other hand, both $\beta 1$ and $\beta 5$ integrins occur in osteoclasts and may have important functions when coupled with αv or other α family integrins that are expressed at lower, but still significant, levels in osteoclasts [24, 25]. There were increases in $\beta 1$ and $\beta 5$ expression in this osteopetrosis with attachment defects, but an abnormally processed form of $\beta 3$ was also a major β chain (Figure 6). However, podosomes did not react with an $\alpha v\beta 3$ monoclonal antibody that labels normal osteoclast podosomes reliably (Figure 4). This probably reflected abnormal processing of $\beta 3$, since $\beta 3$ was mostly smaller than normal (Figure 6). However, the $\beta 3$ sequence was normal in all exons, so we considered an integrin assembly or processing defect. Due to posttranslational processing, integrins in different cell types have different sizes and structures (compare HeLa and MG63 controls to osteoclast lysates in Figure 6). Increased quantities of $\beta 1$ and $\beta 5$ integrin chains also occur with $\beta 3$ defects, although there was no major change in $\alpha 2$ integrin expression, which is reported in Glantzmann's thrombasthenia [13], and the patient had apparently normal clotting function. Thus, the observations were inconsistent with an isolated attachment protein defect.

The key finding, however, in this new type of osteopetrosis was that organization of podosomes lacked the annular structure and association with actin rings that are required for normal osteoclast function (Figure 4). To provide additional insights into a possible molecular defect underlying these findings, we considered that integrin assembly and function in osteoclasts reflects a complex developmental and regulatory system that is required for assembly of the annular integrin ring and for the system to be disassembled for motility. Several proteins contribute to regulation and assembly of the integrin complex. Key elements include the nonreceptor tyrosine kinase Src, the rho family guanine exchange factor Vav3, and the adaptor protein Vasp [9, 11, 26, 27]. Vasp is regulated by the cGMP-dependent protein kinase and is required for motility [27, 28]. Since the cells in this case made pits, albeit small ones, and were motile (Figures 1–2), defects in the proteins Src [29] and Vasp appeared less likely to contribute to the phenotype. However, Vav3 regulates cell spreading and integrin assembly [26]. Study of Vav3 in the osteopetrotic cells showed that Vav3 distribution was dysfunctional. Association with peripheral podosomes and actin organizing structures was totally lost (Figure 5), possibly reflecting an isoform of Vav3 ~ 20 kD smaller than the normal protein (Figure 6). However, as with $\beta 3$, this was not due to defective primary sequence in the exons of the genomic DNA. *av3* deficient mice have increased bone mass, although not frank osteopetrosis [11], although the phenotype is not known in humans. The increased bone mass in Vav3 deficient mice might also reflect possible anabolic effects on bone resorption of non-resorbing osteoclasts [30]. The additional proteins associated with osteoclast organizational defects, *plekhm1* [8] and Src [29], were also sequenced and were normal.

Possible reasons for this phenotype include abnormal regulation of the attachment-detachment cycle, which includes limited proteolytic activity, or an abnormality in an unknown organizing protein upstream of the attachment complex. Proteolytic activity during cell detachment clearly occurs [28], although normally any proteins cleaved should be rapidly cleared and replaced. We cannot exclude the presence of a mutation in introns of $\beta 3$ or Vav3, although it is unlikely. We also cannot exclude a mutation in a regulatory region (promoter, enhancer etc), although this is even less likely since the quantities of proteins produced were normal. In any case, the important membrane integrin assembly complex must involve further elements, and other adaptor protein interactions that cause osteoclastic dysfunction that remain to be described. Although commonly related to absence of the $\beta 3$ integrin, clotting disorders with osteopetrosis are also described with $\alpha 2$ integrins and with $\beta 3$ defects other than deletions [31]. Other candidate integrins regulating osteoclasts include $\alpha 9\beta 1$ [32]. How these, in addition to $\alpha 2$, may affect an osteoclast with an $\alpha \nu \beta 3$ expression defect, are likely related to downstream intermediate proteins and kinases which may vary specifically as integrin assembly specific molecules. Integrin-related pathways beyond Src, Vav3, and Vasp include the integrin-linked kinase [32] and disintegrins including Adam8 [33]. Adam8 is linked to pathological resorption than to deficient resorption [33, 34]. Surface distribution of integrins is also regulated to some extent by the integrin linked kinase [35], and it is expressed in the osteoclast, although its role in modulating adhesion or activity is not known. In macrophages, it is modulated by NF- κ B and linked to NO production [36].

It is also entirely possible, since we sequenced the major genes known to cause related defects directly, that none of the attachment protein complex elements are abnormal. This could also be an epigenomic abnormality, such as microRNA suppression of gene expression, that may mimic a genetic defect. This is presently known in osteoclasts only as a laboratory-created effect [37]. On the other hand, such effects are described with changes in expression due to organ-specific anomalies in micro-RNA expression that affect specific pathways, including integrin expression and cell attachment, in some cells [38, 39]. Such changes in attachment proteins have in been related to cell transformation effects, but there is no reason to believe that similar effects might not affect activity of cells that depend on rapid turnover and replacement of attachment proteins for motility, such as osteoclasts, although this possible mechanism is at present entirely hypothetical.

Importantly, overall assembly of attachment is regulated by the Vav family of guanine nucleotide exchange factors [40, 41, 42]. Although cell-specific defects of integrin assembly related to these elements are not previously described to cause human disease, Vav3 deficient mice have abnormal polarization, increased bone mass, and decreased pit size from osteoclasts made in vitro [11]. The novel type of osteopetrosis described here had abnormal integrin distribution and microscopic resorption pits similar to osteoclasts from the Vav3 deficient mouse. The affected osteoclasts had no peripheral rings of podosomes, and synthesized normal quantities of αv and $\beta 3$ but the $\beta 3$ was processed abnormally. This reflected an abnormal distribution of Vav3, with an abnormal Vav3 isoform at ~70 kD. These findings suggest that truncated Vav3 may be responsible, at least in part, for this new type of human osteopetrosis. However, since the exon sequence of Vav3 was normal, this is either due to an undetected intron defect, or it results from accumulation of partially degraded Vav3 protein. In support of this possibility, a short form of the $\beta 3$ integrin also accumulated. We conclude that, in this new type of osteopetrosis, the integrin organizing complex is dysfunctional, and at least two proteins within the complex included truncated, possibly retained partially degraded, proteins.

Acknowledgements

Supported in part by a N.O.B.E.L. grant from Fondazione Cariplo, and by the Department of Veteran's Affairs (USA) and the National Institutes of Health (USA) AR053976, AR055208, and AR053566.

References

1. Tolar J, Teitelbaum SL, Orchard PJ. Osteopetrosis. *N Engl J Med*. 2004; 351:2839–2349. [PubMed: 15625335]
2. Blair HC, Teitelbaum SL, Ghiselli R, et al. Osteoclastic bone resorption by a polarized vacuolar proton pump. *Science*. 1989; 245:855–857. [PubMed: 2528207]
3. Li YP, Chen W, Liang Y, et al. Atp6i-deficient mice exhibit severe osteopetrosis due to loss of osteoclast-mediated extracellular acidification. *Nat Genet*. 1999; 23:447–451. [PubMed: 10581033]
4. Blair HC, Borysenko CW, Villa A, et al. In vitro differentiation of CD14 cells from osteopetrotic subjects: contrasting phenotypes with TCIRG1, CLCN7, and attachment defects. *J Bone Miner Res*. 2004; 19:1329–1338. [PubMed: 15231021]
5. Scheel O, Zdebik AA, Lourdel S, et al. Voltage-dependent electrogenic chloride/proton exchange by endosomal CLC proteins. *Nature*. 2005; 436:424–427. [PubMed: 16034422]
6. Kornak U, Kasper D, Bosl MR, et al. Loss of the ClC-7 chloride channel leads to osteopetrosis in mice and man. *Cell*. 2001; 104:205–215. [PubMed: 11207362]

7. Lange PF, Wartosch L, Jentsch TJ, et al. CIC-7 requires Ostm1 as a beta-subunit to support bone resorption and lysosomal function. *Nature*. 2006; 440:220–223. [PubMed: 16525474]
8. Van Wesenbeeck L, Odgren PR, Coxon FP, et al. Involvement of PLEKHM1 in osteoclastic vesicular transport and osteopetrosis in incisors absent rats and humans. *J Clin Invest*. 2007; 117:919–930. [PubMed: 17404618]
9. Blair HC, Zaidi M. Osteoclastic differentiation and function regulated by old and new pathways. *Rev Endocr Metab Disord*. 2006; 7:23–32. [PubMed: 17115268]
10. Sobacchi C, Frattini A, Guerrini MM, et al. Osteoclast-poor human osteopetrosis due to mutations in the gene encoding RANKL. *Nat Genet*. 2007; 39:960–962. [PubMed: 17632511]
11. Faccio R, Teitelbaum SL, Fujikawa K, et al. Vav3 regulates osteoclast function and bone mass. *Nat Med*. 2005; 11:284–290. [PubMed: 15711558]
12. Guerrini MM, Sobacchi C, Cassani B, et al. Human osteoclast-poor osteopetrosis with hypogammaglobulinemia due to TNFRSF11A (RANK) mutations. *Am J Hum Genet*. 2008; 83:64–76. [PubMed: 18606301]
13. Horton MA, Massey HM, Rosenberg N, et al. Upregulation of osteoclast $\alpha 2\alpha 1$ integrin compensates for lack of $\alpha v\alpha 3$ vitronectin receptor in Iraqi-Jewish-type Glanzmann thrombasthenia. *Br J Haematol*. 2003; 122:950–957. [PubMed: 12956766]
14. Frattini A, Orchard PJ, Sobacchi C, et al. Defects in TCIRG1 subunit of the vacuolar proton pump are responsible for a subset of human autosomal recessive osteopetrosis. *Nat Genet*. 2000; 25:343–346. [PubMed: 10888887]
15. Robinson LJ, Yaroslavskiy BB, Griswold RD, et al. Estrogen inhibits RANKL-stimulated osteoclastic differentiation of human monocytes through estrogen and RANKL-regulated interaction of ER- α with BCAR1 and Traf6. *Exp Cell Res*. 2009; 315:1287–1301. [PubMed: 19331827]
16. Yaroslavskiy BB, Li Y, Ferguson DJP, Kalla SE, et al. Autocrine and Paracrine Nitric Oxide Regulate Attachment of Human Osteoclasts. *J Cell Biochem*. 2004; 91:962–972. [PubMed: 15034931]
17. Carano A, Schlesinger PH, Athanasou NA, et al. Acid and base effects on avian osteoclast activity. *Am J Physiol*. 1993; 264:C694–C701. [PubMed: 8460672]
18. Kudo O, Fujikawa Y, Itonaga I, et al. Proinflammatory cytokine (TNF α / IL-1 α) induction of human osteoclast formation. *J Pathol*. 2002; 198:220–227. [PubMed: 12237882]
19. Frattini A, Vezzoni P, Villa A, et al. The dissection of human autosomal recessive osteopetrosis identifies an osteoclast-poor form due to RANKL deficiency. *Cell Cycle*. 2007; 6:3027–3033. [PubMed: 18202550]
20. Blair HC, Athanasou NA. Recent advances in osteoclast biology and pathological bone resorption. *Histol Histopathol*. 2004; 19:189–199. [PubMed: 14702187]
21. Ross FP, Chappel J, Alvarez JI, et al. Interactions between the bone matrix proteins osteopontin and bone sialoprotein and the osteoclast integrin $\alpha v\beta 3$ potentiate bone resorption. *J Biol Chem*. 1993; 268:9901–9907. [PubMed: 8486670]
22. Roux S, Pichaud F, Quinn J, et al. Effects of prostaglandins on human hematopoietic osteoclast precursors. *Endocrinology*. 1997; 138:1476–1482. [PubMed: 9075705]
23. Bader BL, Rayburn H, Crowley D, et al. Extensive vasculogenesis, angiogenesis, and organogenesis precede lethality in mice lacking all αv integrins. *Cell*. 1998; 95:507–519. [PubMed: 9827803]
24. Nakayama S, Okada Y, Saito K, et al. $\beta 1$ integrin/focal adhesion kinase-mediated signaling induces intercellular adhesion molecule 1 and receptor activator of nuclear factor κB ligand on osteoblasts and osteoclast maturation. *J Biol Chem*. 2003; 278:45368–45374. [PubMed: 12954625]
25. Sago K, Teitelbaum SL, Venstrom K, et al. The integrin $\alpha v\beta 5$ is expressed on avian osteoclast precursors and regulated by retinoic acid. *J Bone Miner Res*. 1999; 14:32–38. [PubMed: 9893063]
26. Felsenfeld DP, Schwartzberg PL, Venegas A, et al. Selective regulation of integrin-cytoskeleton interactions by the tyrosine kinase Src. *Nat Cell Biol*. 1999; 1:200–206. [PubMed: 10559917]
27. Yaroslavskiy BB, Zhang Y, Kalla SE, et al. NO-dependent osteoclast motility: reliance on cGMP-dependent protein kinase I and VASP. *J Cell Sci*. 2005; 118:5479–5487. [PubMed: 16291726]

28. Yaroslavskiy BB, Sharrow AC, Wells A, et al. Necessity of inositol (1,4,5)-trisphosphate receptor 1 and mu-calpain in NO-induced osteoclast motility. *J Cell Sci.* 2007; 120:2884–2894. [PubMed: 17690304]
29. Miyazaki T, Tanaka S, Sanjay A, et al. The role of c-Src kinase in the regulation of osteoclast function. *Mod Rheumatol.* 2006; 16:68–74. [PubMed: 16633924]
30. Karsdal MA, Martin TJ, Bollerslev J, et al. Are nonresorbing osteoclasts sources of bone anabolic activity? *J Bone Miner Res.* 2007; 22:487–494. [PubMed: 17227224]
31. Yarali N, Fisqin T, Duru F, et al. Osteopetrosis and Glanzmann's thrombasthenia in a child. *Ann Hematol.* 2003; 82:254–256. [PubMed: 12707732]
32. Boulter E, Van Obberghen-Schilling E. Integrin-linked kinase and its partners: a modular platform regulating cell-matrix adhesion dynamics and cytoskeletal organization. *Eur J Cell Biol.* 2006; 85:255–263. [PubMed: 16546570]
33. Mandelin J, Li TF, Hukkanen MV, et al. Increased expression of a novel osteoclast-stimulating factor, ADAM8, in interface tissue around loosened hip prostheses. *J Rheumatol.* 2003; 30:2033–2038. [PubMed: 12966612]
34. Ainola M, Li TF, Mandelin J, et al. Involvement of ADAM8 in osteoclastogenesis and pathological bone destruction. *Ann Rheum Dis.* (in press).
35. Vouret-Craviari V, Boulter E, Grall D, et al. ILK is required for the assembly of matrix-forming adhesions and capillary morphogenesis in endothelial cells. *J Cell Sci.* 2004; 117:559–569. [PubMed: 14709721]
36. Tan C, Mui A, Dedhar S. Integrin-linked kinase regulates inducible nitric oxide synthase and cyclooxygenase-2 expression in an NF- κ B-dependent manner. *J Biol Chem.* 2002; 277:3109–3116. [PubMed: 11724787]
37. Sugatani T, Hruska KA. Impaired micro-RNA pathways diminish osteoclast differentiation and function. *J Biol Chem.* 2009; 284:4667–4678. [PubMed: 19059913]
38. Müller DW, Bosserhoff AK. Integrin beta 3 expression is regulated by let-7a miRNA in malignant melanoma. *Oncogene.* 2008; 27:6698–6706. [PubMed: 18679415]
39. Brendle A, Lei H, Brandt A, et al. Polymorphisms in predicted microRNA-binding sites in integrin genes and breast cancer. *Carcinogenesis.* 2008; 29:1394–1399. [PubMed: 18550570]
40. Miranti CK, Leng L, Maschberger P, et al. Identification of a novel integrin signaling pathway involving the kinase Syk and the guanine nucleotide exchange factor Vav1. *Curr Biol.* 1998; 8:1289–1299. [PubMed: 9843681]
41. Ardouin L, Bracke M, Mathiot A, et al. Vav1 transduces TCR signals required for LFA-1 function and cell polarization at the immunological synapse. *Eur J Immunol.* 2003; 33:790–797. [PubMed: 12616499]
42. Graham DB, Robertson CM, Bautista J, et al. Neutrophil-mediated oxidative burst and host defense are controlled by a Vav-PLCgamma2 signaling axis in mice. *J Clin Invest.* 2007; 117:3445–3452. [PubMed: 17932569]

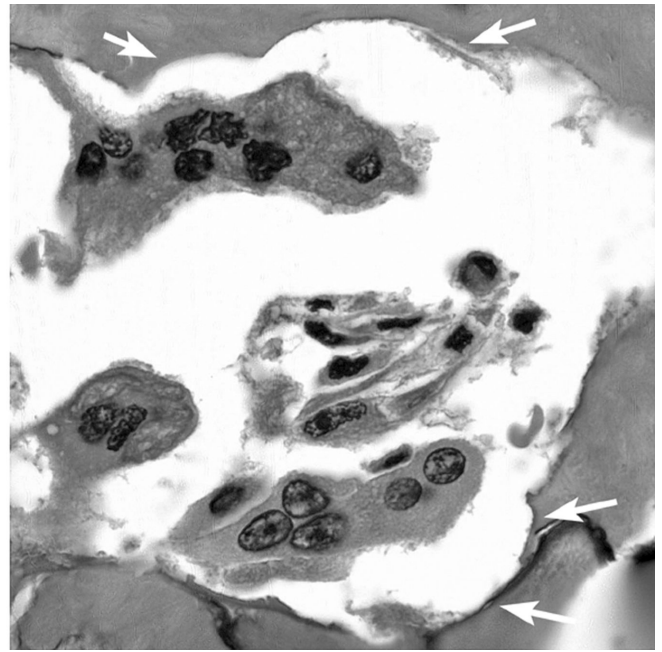
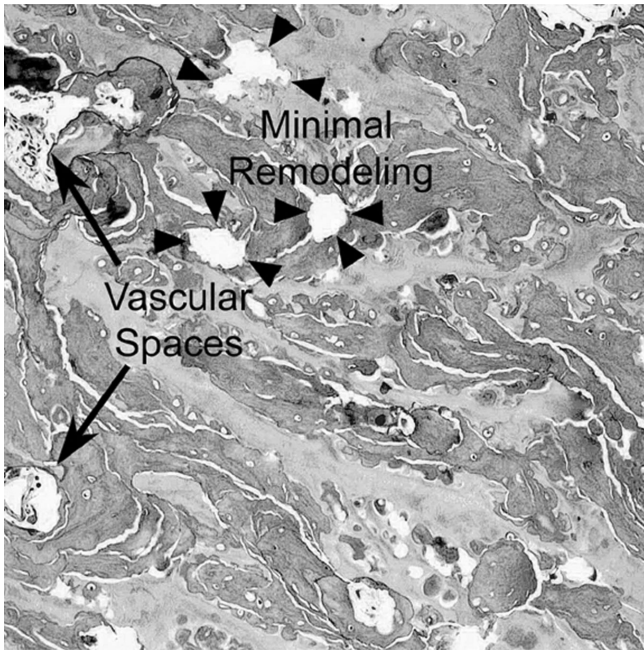


Figure 1. Features of bone from a biopsy of the iliac crest

A. Severe osteopetrosis with minimal remodeling including some vascular spaces.

Although the subject survived for 28 years prior to transplant, the major part of the bone was retained cartilage (lightly stained acellular material) with the balance mainly composed of primary spongiosa, and a few spaces. Low power (10× objective); the field shown is 800 μm across.

B. Osteoclasts with shallow resorptive pits. Osteoclasts were present and appeared normal by light microscopy, although pits were small and shallow relative to the number of multinucleated cells present. High power (40× objective); the field shown is 110 μm across.

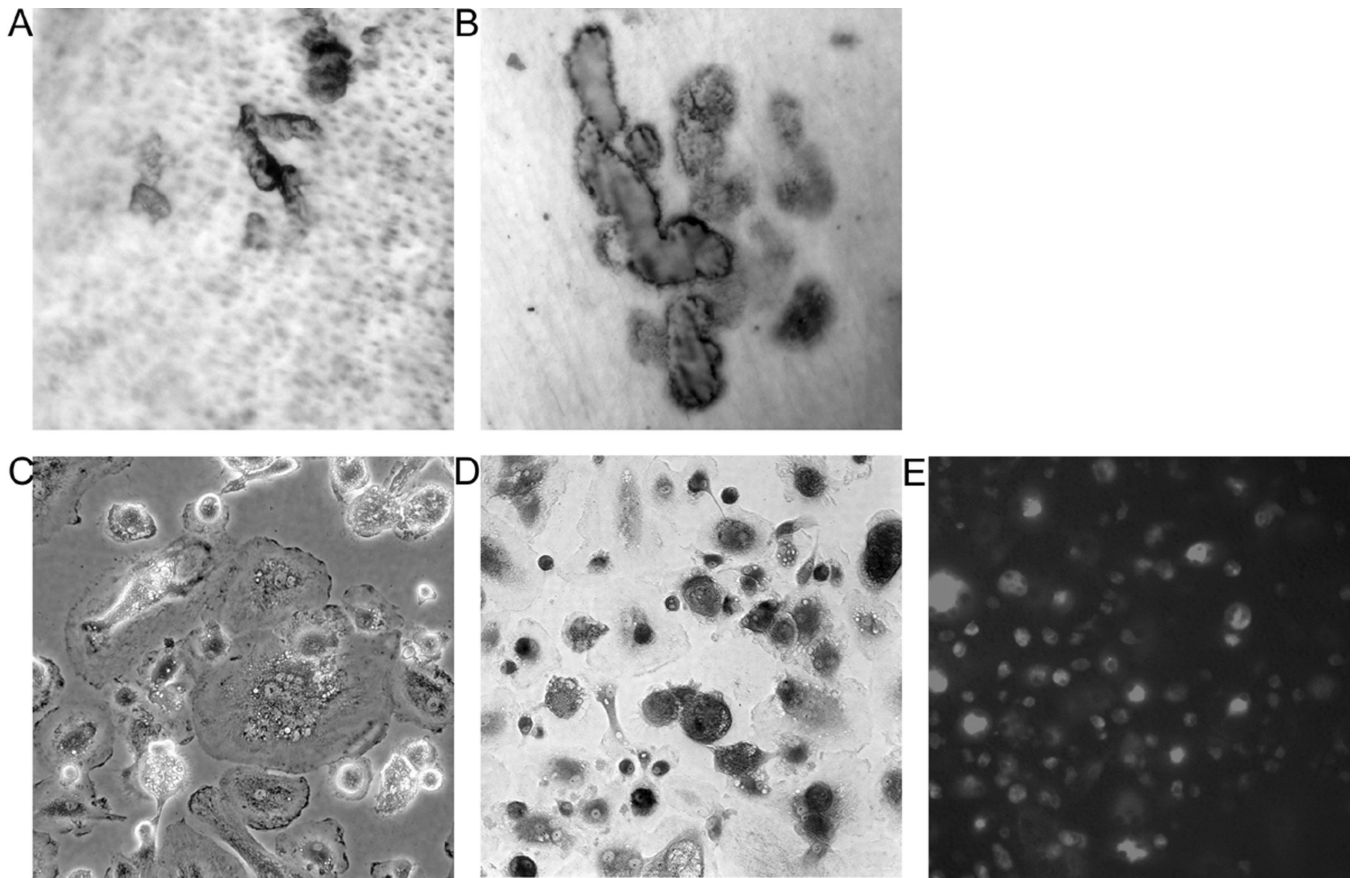


Figure 2. Osteoclasts formed in vitro from osteopetrotic monocytes make small pits but have normal multinucleation and tartrate resistant acid phosphatase expression

A–B Pit assays from osteopetrotic and control osteoclasts. Osteoclasts from the osteopetrotic patient produced pits (A), but the pits averaged 10–15 μm in diameter, much smaller than the osteoclasts themselves (Figure 1 and C–D below). Control osteoclasts produced pits averaging 40 μm in diameter (B). Fields 450 μm across (20 \times objective) are shown. Cells produced in vitro were incubated on whale dentine for 12 days. The substrate was cleaned by sonication and labeled with toluidine blue to show partially degraded matrix proteins at pit sites.

C. Osteopetrotic osteoclasts in vitro. Phase microscopy showed large multinucleated cells, typical of RANKL stimulated cell differentiation in vitro. The field shown is 280 μm across.

D. tartrate-resistant acid phosphatase activity of osteopetrotic osteoclasts formed in vitro. Tartrate resistant acid phosphatase activity was completely typical of osteoclasts in vitro. This frame a bright-field image 450 μm across, the same magnification as A and B. Note that the pits in B have similar sizes to the large rounded cells expressing large amounts of TRAP, but that the pits in A are much smaller (see also Figure 1B).

E. Lysotracker red DND labeling. Cells on glass contain abundant acidic vacuoles, the same as in normal osteoclasts (not illustrated) [4]. The field is 450 μm across.

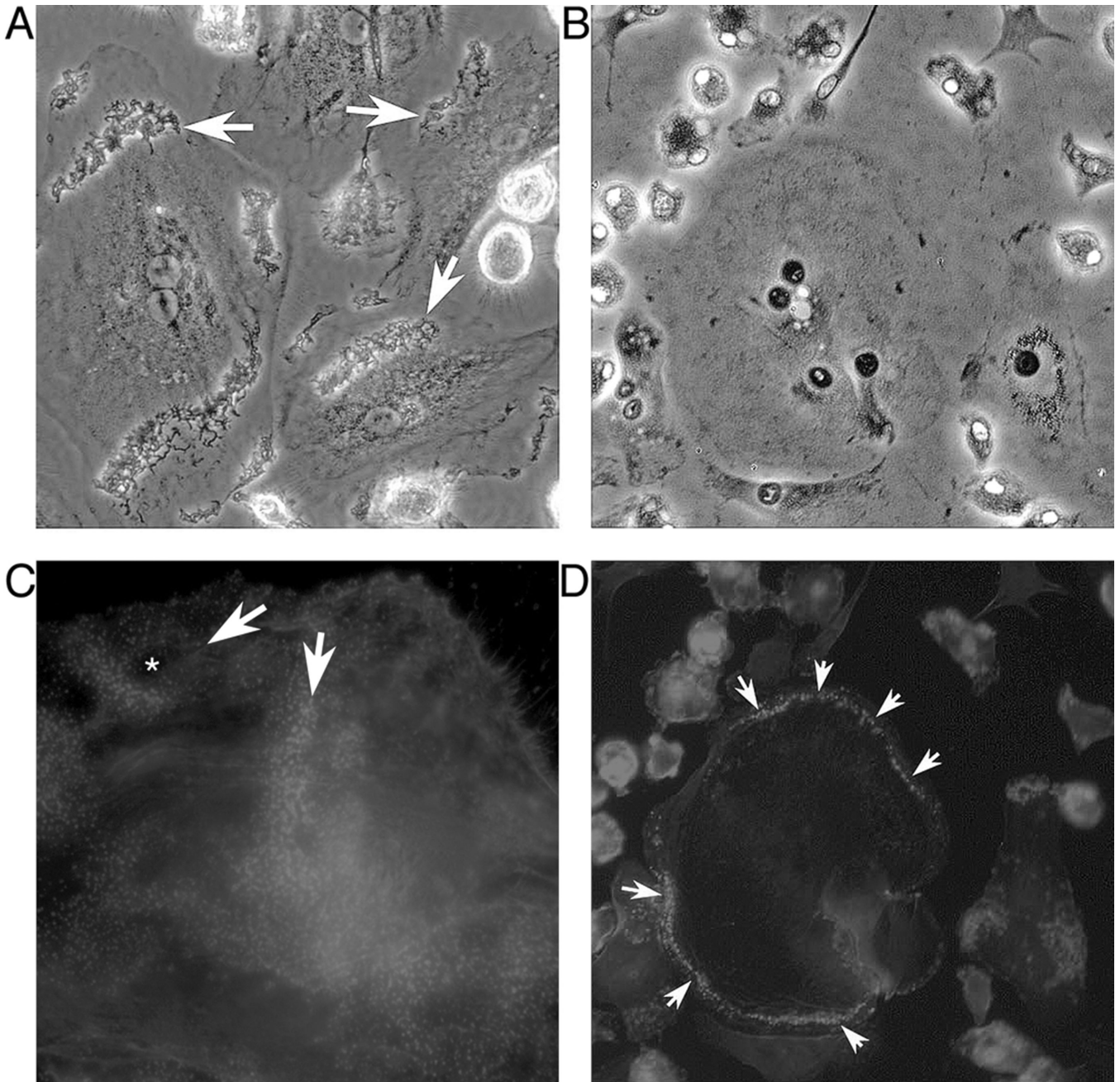


Figure 3. High resolution phase and phalloidin rhodamine labeling show podosomal anomalies in osteopetrotic osteoclasts

Cells were grown on glass cover slips. The fields shown were taken with 40× objectives and all photographs are 220 μm across.

A, C. Osteoclasts from the osteopetrotic patient. In phase contrast at high power (A) prominent cell membrane structures often occurred in broad regions of the cells (arrows). Phalloidin rhodamine labeling (C) showed very large clusters and bands of podosomes sometimes in peripheral bands and in some cases across the center of the cell attachment (arrows). These ringed some spaces (asterisk) but typically these were much smaller than the cell diameters, and highly variable. A and C are photographs of two similar fields.

B, D. Control normal osteoclasts showing peripheral cell attachment structure. In contrast to osteopetrotic cells, normal osteoclasts have well defined borders in phase (B) that correspond to one or more regular and well defined peripheral rings of podosomes (Arrowheads, D). The cells shown in B and D are the same field.

Author Manuscript

Author Manuscript

Author Manuscript

Author Manuscript

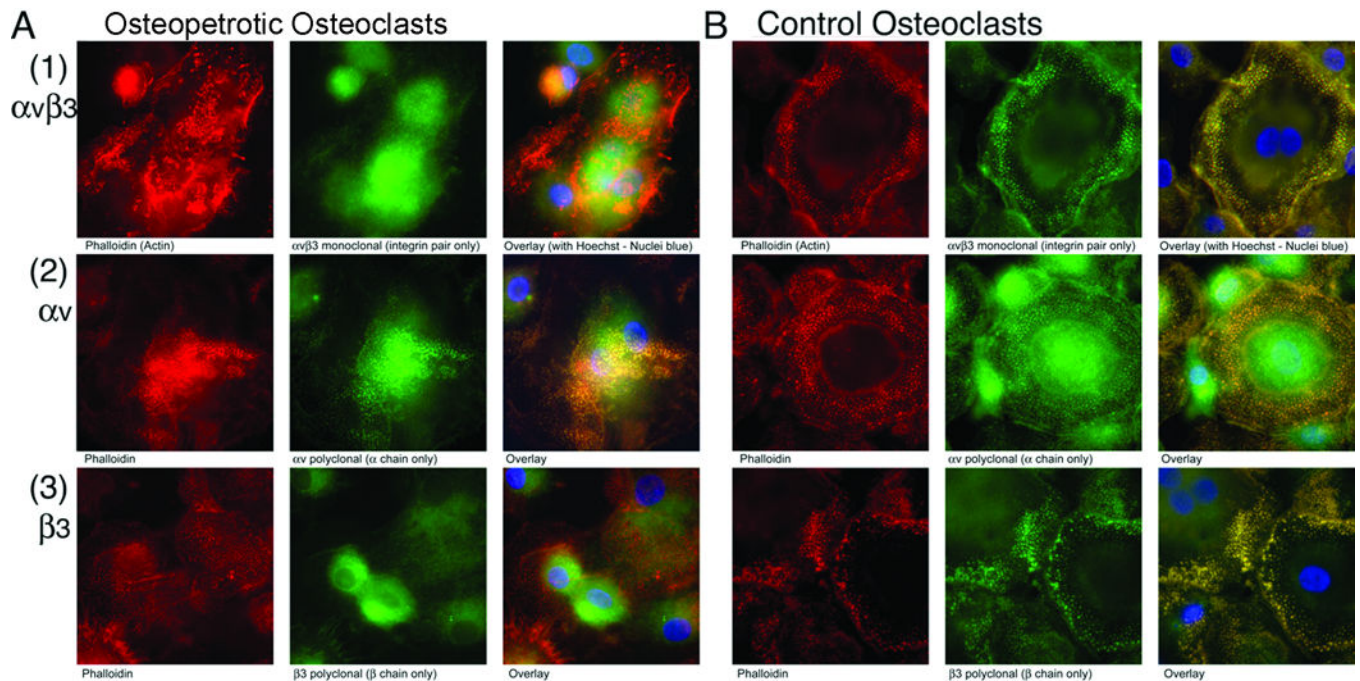


Figure 4. Integrin distribution in control and osteopetrotic osteoclasts

Cells grown as in Figures 1–2 were labeled for actin (phalloidin, red), antibodies to integrins specified (green), and Hoechst dye (nuclei, blue). Fields are each 85 μ m across.

A. Podosomes from osteoclasts of the affected subject label poorly for α v β 3 integrin or β 3 subunits, but include α v integrin. The left column (red) shows actin with prominent podosomes in abnormal distribution (larger fields shown in Figure 3). Monoclonal antibody for the α v β 3 pair (**1, top row**) and polyclonal antibodies to α v (**2, middle row**) and β 3 N-terminal (**3, bottom row**) were used to label integrins (second column, green). There was essentially no colocalization α v β 3 with podosomes (third column, yellow shows colocalization). Labeling with anti-N-terminal β 3 was weak and did not colocalize with actin. This may reflect degradation of the β 3 C-terminal (see Figure 6). There was colocalization of α v with podosomes (third column from left), although podosomes were abnormally distributed as in Figure 3.

B. Podosomes from normal osteoclasts label for α v β 3 integrin, and for α v or β 3 integrin subunits. The photographs parallel those of the osteopetrotic cells (A). The osteoclasts have prominent peripheral rings of podosomes that label well with the integrin pair and with each integrin subunit (yellow in merged images, right column). No labeling of control or osteopetrotic cells for α 2 integrin was detected in similar assays (not shown; α 2 integrin is not expressed in major amounts in these cells, see Figure 6).

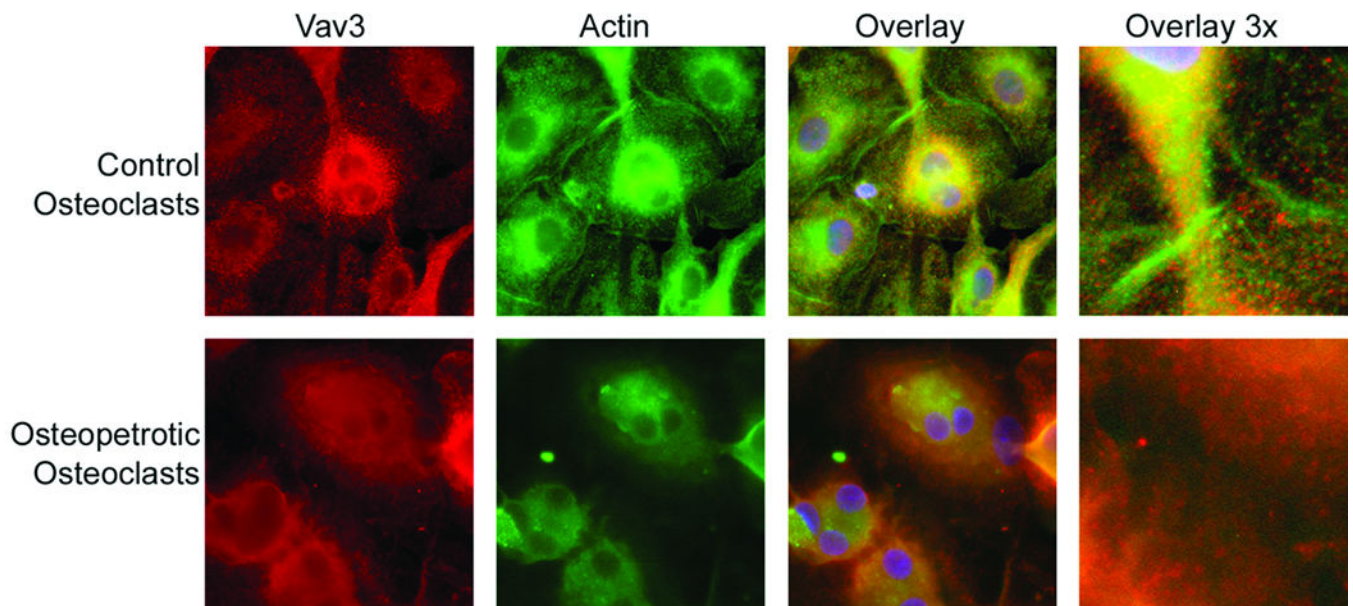


Figure 5. Dysfunctional distribution of Vav3 in osteopetrotic cells with abnormal attachment
Vav3 is critical to the organization of the cellular attachment and membrane receptors. Vav3 is associated with attachment structures in the periphery of control cells (top row). Vav3 was not associated with actin or podosomes in the periphery of osteopetrotic cells (bottom row). The relationship of Vav3, around the periphery of podosomes and near actin filaments, is seen most clearly at very high magnification power (right frames, 30 μm across). Other frames are 85 μm square.

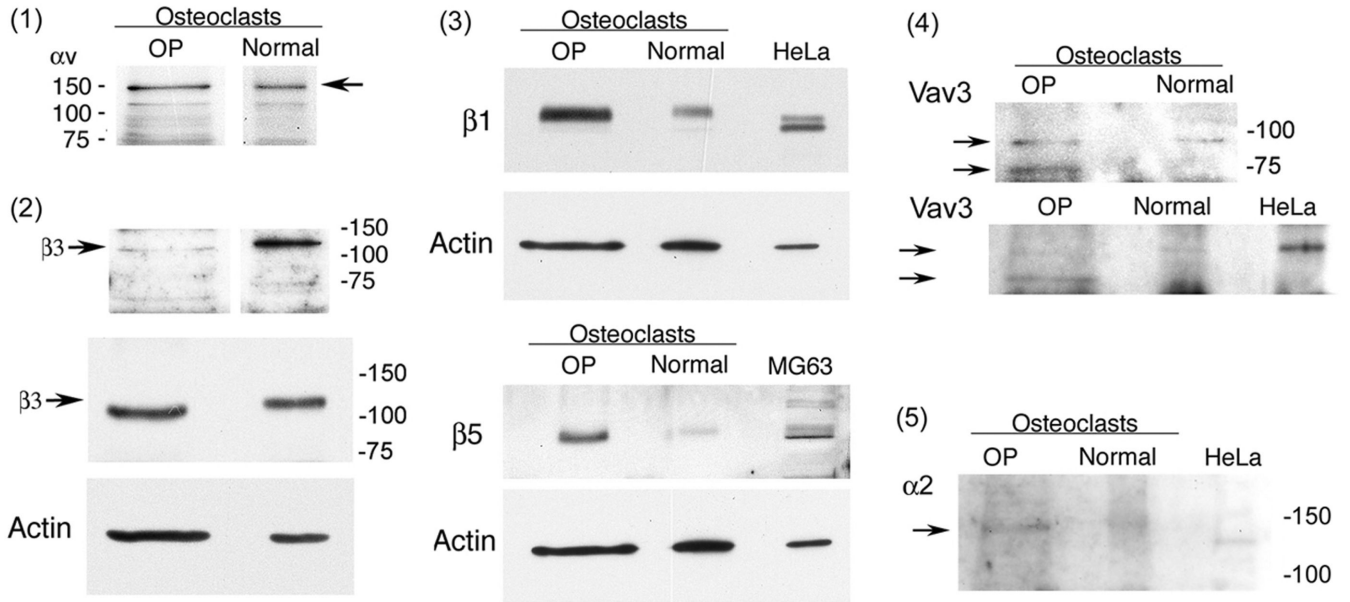


Figure 6. Western blots for integrin subunits and Vav3 in osteopetrotic osteoclasts and control cells

Blots used 10 μ g of cell lysate protein separated on 8 or 10% SDS-PAGE and polyclonal antibodies visualized by enhanced chemiluminescence (see Methods).

(1) Control and osteopetrotic cells showed similar results with antibody to the αv integrin subunit. (2) Re-blot of the membrane (1) for the C terminal region of the $\beta 3$ subunit was very weak in the osteopetrotic patient. A second blot using an antibody to the $\beta 3$ subunit N terminal region was showed similar $\beta 3$ in control and osteopetrotic cell (OP) cell lysates, although the $\beta 3$ is probably differently processed since its nucleotide sequence was normal (see text). Actin re-blot is shown as a protein loading control in the second blot. Under the conditions used, actin is near the front and OP lysates, which contained more salt than controls, expanded toward the front.

(3) Osteoclasts with $\beta 3$ defects have compensatory increases in $\beta 1$ or $\beta 5$. Additional blots using HeLa cells as a positive control for $\beta 1$ and MG63 cells as a control for $\beta 5$, since these integrin chains are expressed at low levels in normal osteoclasts. Both $\beta 1$ and $\beta 5$ were present in higher amounts in osteopetrotic cells than in normal controls.

(4) Re-blots of membranes from (1) and (3) for Vav3. The OP patient showed two isoforms, one ~20 kD smaller than the normal form, which is also abundant in the HeLa cells.

(5) The $\alpha 2$ integrin subunit is a minor protein, barely detectable, in normal or OP osteoclasts. Re-blot of the membrane in (3) upper panel. This is in keeping with normal αv expression, but contrasts with findings in patients with isolated $\beta 3$ defects (see text). Re-blot of (3).

Table 1**Primers for sequencing**

Primers were designed in the flanking introns (or in flanking regions for the first and last primers). Sequences are from GenBank; the header of each section is the GenBank gene name; the sequences are from that gene file for *Homo sapiens*.

Gene symbol		
Exon/	Forward Primer	Reverse Primer
SRC		
1	GGGCTCGTTTTCCCTATCT	CCAGGCAACGAAAAAGGACT
2	CACGGATGCAGTGGACACGT	GATACTTGGGTGGGCTGACG
3-4	AGATGACCAAGGCCAGTCCT	ATCCTGCCATTACCTCCACC
5	CCTCCCTCCCTCCAATGTC	GTCCCCACCCTTCTAGGCTC
6	TGCGTGTCCCCTGAAATCTG	GTCACCAGCCCCATTACAG
7	TAACAGTGCCATGAGGAGCA	CTACTTGGGTGGCTGAGGTG
8	TCTGCTGTGCTGGTTAAAGC	GTAAATACGTGCGGCAAGAT
9-10	GAAGAAGTGTGGGGAGGGTG	GCCTAACATCAGACGCTCAA
11	TTGAGCGTCTGATGTTAGGC	CCCACAGAGAGAGGACCAAC
VAV3		
1	GGGACCCCATCGTATTACAG	CGCATGATTAATGGGAGCTG
2	AAAGGCTGCTTGATGCTTTC	TGGTTTTGCTAAGCCATCTACA
3	GCCCTTCTCATTCTGCACAT	AAGAAGAACCACACCAGTGACA
4	GAGCAGAAATGTCAGGGTCA	AAAACCCACAATGGACACAT
5	CACTGCCCTCGTTATTGGAT	GGTCATGCATATGTCTCCAAA
6	CAGCAAAGATGCCTCACAAA	CTGAAACAGTGCCACTCAGG
7	TCCTTCCTTTTGAAGCATT	GGAACCCCTAAGGAAATGA
8	CCTGAGTGGCAAGTCTAGCA	TGAAAGTAATTGTCCCAGTTC
9	GTTTCCCCTCCAGTTCATT	CATGTAAAACACAGGGCCATAA
10	CCTAGGGCCTTTCATCTTT	GGCAGCTACTGACCATCTCTG
11	GGAAATGGAGCCCAGACATA	CCATGCAAGGATAACTATTCCA
12	GCTTTGATTGACTGGGCATT	GGGACAAGCCATCACAAAGT
13	ACCCTTCCGGTTGAGTCTTT	TTCCCCTACTTCACACTGG
14-15	CCCCGTTGTTTTTCAGTGTATG	TCCCGTCGCTGTACACATTA
16-17	TTGAGCTTTGTTGTGAAAC	CCATCCAACCTCCCTTTGAA
18	GCATGTTGAAAGAAAGTTGC	CCTTCGGACAGTGACAGTGA
19	TGCTTTCCAAAGTGCCAGTA	AGGGTGCTGGATATGTGAGC
20	TGTCAGGGATCATGGGATAAA	TGCTTTGCACTGTGGACTC
21	TTGCTTCCTTTTCTGATCCAC	TGACCTGGCCAGTATCCTTT
22	GTTCCAGGACTGTGCCACTT	AGCCGAGACAAATGGAAATG
23-24	GCCTCTGTCTCTCCAGGT	TGAAGATTACGATTCGAGCA
25	TCCAGACAGCAGGGAGAGAT	GCCTGTTGGTCCATCTGACT
26-27	CGAACTGCAAACCTACTGTCA	TGTTGAACAGCCAGAAATGC
PLEKHM1	As reported [8]	

<u>Gene symbol</u>		
<u>Exon/</u>	<u>Forward Primer</u>	<u>Reverse Primer</u>
ITGB3		
1	GGCGAGAGAGGAGCAAAGTT	GCTCCA AGTCCGCAACTTGAC
2	GCAAGTACCTTCACTGAGCCA	AGGGAGGTGATAACTTCATGG
3	GGTAGAGAGTCGCCATAGTTC	CAAGACTTCTCCTCAGACCT
4	CCCAACTGTATCCAAATCTGC	AACCAGGACTTGGACCTTCCT
5	TCCCCTCTCTTCCCTTCCCAA	TTCAGTCACTTCCTTTCCAG
6	TCTTACCAGTGACATGGCTG	CTCTGCCTAGATTAGGGCAAC
7	GCAGCCCGAAGCAAGATAAGT	TGGGGACTGTATCCAATGCTA
8	GCTTTTGGAGACCACCAGCTT	AGCCCTGCTGTGTAAGCCAAA
9	TGCTCTTGCAATTCCTGTTTC	GGGGCCATTTTATGCACTAC
10	GGCCCAACTGTGTCTAAATAC	TGCAGGTATATGAGGGGGTGT
11–12	TGTGTAGCCTGCTGCCATGGA	ACCTGGGTGTGTGCAACTCTA
12	GATCAGAGCTGGACTGGGATA	ACCTGGGTGTGTGCAACTCTA
13	GTTTGGAGTGGTCCCATCTTC	GAGATTCCTGCCTAACATGGT
14	GGACCTTAGTTACTTTGTC	ATCTCTCCAGTTTCCAGA
15	AGAGAACGGTGCCTTGGGAAA	ACACACTCCACACACAACAC